Study of the induced potential produced by ultrashort pulses on metal surfaces

Marisa Faraggi,[1,*] Iñigo Aldazabal,[1,2] Maria Silvia Gravielle,[3] Andres Arnau,[2,4] and Vyacheslav M. Silkin[1,4,5]

[1]*Donostia International Physics Center (DIPC), Paseo de Manuel Lardizabal 4, 20018 San Sebastián, Spain*
[2]*Centro de Física de Materiales CFM-MPC, Centro Mixto (CSIC-UPV/EHU), San Sebastián, Spain*
[3]*Instituto de Astronomía y Física del Espacio, CONICET, C. C. 67, Sucursal 28, 1428 and Departamento de Física, FCEN-UBA, Buenos Aires, Argentina*
[4]*Departamento de Física de Materiales, Facultad de Química UPV/EHU, San Sebastián, Spain*
[5]*IKERBASQUE, Basque Foundation for Science, 48011 Bilbao, Spain*
**Corresponding author: faraggi@iafe.uba.ar*

Received September 18, 2009; accepted October 7, 2009;
posted October 23, 2009 (Doc. ID 116656); published November 17, 2009

The relevance of the induced potential for photoelectron emission from metal surfaces resulting from grazing-incidence ultrashort laser pulses is studied. To describe this process we introduce a distorted-wave method, which includes the perturbation on the emitted electron produced by both the laser and the induced fields. The method is applied to an Al(111) surface, and the results are compared with the numerical solution to the time-dependent Schrödinger equation. We find that our approach reproduces the main features of emission spectra well, accounting properly for effects originated by the induced potential. © 2009 Optical Society of America

OCIS codes: 240.6700, 260.7120, 260.5210.

1. INTRODUCTION

In the past few years developments in laser technology have made possible the production of laser pulses with durations on the subfemtosecond scale [1–5]. This advance in the experimental area opens up new branches in research in matter–radiation systems [6–11], including the dynamics of collective excitations [12,13]. In particular, the investigation of photoelectron emission from surfaces that is due to the incidence of short laser pulses provides a chance to understand a piece of the complicated puzzle corresponding to electron dynamics at metal surfaces.

In this paper we investigate the photoelectron emission produced when an ultrashort laser pulse impinges grazingly on a metal surface, focusing attention on the role played by the surface induced potential. The induced potential is caused by the rearrangement of valence-band electrons due to the presence of the external electromagnetic field. This potential is not expected to affect electron emission appreciably for high frequencies of the laser pulse, for which surface electrons are not able to follow the fast fluctuations of the field. But for frequencies of the pulse close to or lower than the surface plasmon frequency, the induced potential becomes comparable with the laser perturbation, and its effect cannot be neglected. We introduce a simple model, named the surface jellium–Volkov (SJV) approximation, which includes information about the action of the surface induced potential, taking into account the main features of the process.

The SJV approach is a time-dependent distorted wave method that uses the well-known Volkov phase [14] to describe the interaction of the active electron with the laser and the induced fields, while the surface potential is represented within the jellium model. This kind of one-active-electron theory has recently been applied to study different laser-induced electron emission processes from metal surfaces, providing reasonable predictions [15–18]. To corroborate the validity of the proposed approximation, we compare SJV results with the numerical solution of the time-dependent Schrödinger equation (TDSE), in which the contribution of the surface induced potential is also included. The induced potential is here obtained from a linear response theory by considering a jellium model for a one-dimensional slab. It is worth noting that, in contrast to the TDSE method, the SJV model gives us the possibility of studying each mechanism separately, with a low computational cost.

With both methods—SJV and TDSE—we calculate the probability of electron emission from the valence band of an Al surface, considering different frequencies and durations of the laser pulse. We analyze in detail the effect of the induced potential on electron distributions by comparing values derived from the previous impulsive jellium–Volkov (IJV) approximation [16], which does not contain the dynamic response of the surface.

The paper is organized as follows. In Section 2 we present the theory, in Section 3 results are shown and discussed, and finally in Section 4 conclusions are summarized. Atomic units are used throughout unless otherwise stated.

2. THEORY

Let us consider a laser pulse impinging grazingly on a metal surface (S). As a consequence of the interaction, an electron (e) of the valence band of the solid, initially in the state i, is ejected above the vacuum level, ending in a final state f. The frame of reference is placed at the position of

the crystal border, with the $\hat{z}$ axis perpendicular to the surface, pointing toward the vacuum region.

For this collision system we can write the Hamiltonian corresponding to the interacting electron as

$$H = H_0 + V_L + V_{\text{ind}}, \tag{1}$$

where $H_0 = -\nabla_{\mathbf{r}}^2/2 + V_S$ is the unperturbed Hamiltonian, with V_S the electron–surface potential, and $V_L = \mathbf{r}\cdot\mathbf{F}(t)$ represents the electron interaction with the laser field $\mathbf{F}(t)$ at the time t, expressed in the length gauge. In Eq. (1), V_{ind} denotes the surface induced potential, which is originated by electronic density fluctuations produced by the external field.

The electron interaction with the surface, V_S, is here described with the jellium model, being $V_S = -V_c\Theta(-z)$ with $V_c = E_F + E_W$, where E_F is the Fermi energy, E_W is the work function, and Θ denotes the unitary Heaviside function. This simple surface model has proved to give an adequate description of the electron–surface interaction for electron excitations from the valence band of metal surfaces [16–19]. Within the jellium model the unperturbed electronic states, eigenstates of H_0, are written as

$$\Phi_{\mathbf{k}}^{\pm}(\mathbf{r},t) = \frac{e^{i\mathbf{k}_s\cdot\mathbf{r}_s}}{2\pi}\varphi_{k_z}^{\pm}(z)e^{-iE_{\mathbf{k}}t}, \tag{2}$$

where the position vector of the active electron e is expressed as $\mathbf{r} \equiv (\mathbf{r}_s, z)$, with $\mathbf{r}_s$ and z the components parallel and perpendicular to the surface, respectively. The vector $\mathbf{k} = (\mathbf{k}_s, k_z)$ is the momentum measured inside the solid, and $E_{\mathbf{k}} = k_s^2/2 + \varepsilon_{k_z}$ corresponds to the electron energy. The signs $\pm$ define the outgoing $(+)$ and incoming $(-)$ asymptotic conditions of the collision problem, and the eigenfunctions $\varphi_{k_z}^{\pm}(z)$ with eigenenergy ε_{k_z} are given in the appendix of [20].

Taking into account the grazing-incidence condition, together with the translational invariance of V_S in the direction parallel to the surface, we choose the electric field $\mathbf{F}(t)$ perpendicular to the surface plane, that is, along the $\hat{z}$ axis. The temporal profile of the pulse is defined as

$$F(t) = F_0 \sin(\omega t + \phi)\sin^2(\pi t/\tau) \tag{3}$$

for $0 < t < \tau$ and 0 elsewhere, where F_0 is the maximum field strength, ω is the carrier frequency, ϕ represents the carrier envelope phase, and τ determines the duration of the pulse.

The differential probability of electron emission from the surface is expressed in terms of the transition matrix as

$$\frac{dP}{d\mathbf{k}_f'} = \rho_e \frac{k_{fz}'}{k_{fz}} \int d\mathbf{k}_i \Theta(v_F - k_i)|T_{if}|^2, \tag{4}$$

where T_{if} is the T-matrix element corresponding to the inelastic transition $\mathbf{k}_i \to \mathbf{k}_f'$ and $\mathbf{k}_f' = (\mathbf{k}_{fs}, k_{fz}')$ is the final electron momentum outside the solid, with $k_{fz}' = (k_{fz}^2 - 2V_c)^{1/2}$. In Eq. (4), $\rho_e = 2$ takes into account the spin states, and Θ restricts the initial states to those contained within the Fermi sphere, with $v_F = (2E_F)^{1/2}$. The angular distribution of emitted electrons can be derived in a straightforward way from Eq. (4) as $d^2P/dE_f d\Omega_f = k_f' dP/d\mathbf{k}_f'$, where E_f and Ω_f are the final energy and the solid angle, respectively, of the ejected electron and $k_f' = |\mathbf{k}_f'|$.

In this work we evaluate T_{if} by using two different methods: the SJV approximation and the numerical solution of the TDSE. Both of them are summarized below.

A. Surface Jellium–Volkov Approximation

In the SJV theory, the final distorted state is represented by the SJV wave function, which includes the actions of the laser field and the induced potential on the emitted electron, both described by means of the Volkov phase. The Volkov phase is derived from the exact solution of a free electron within an electric potential and takes into account the distortion of the electronic state produced by the external field. This approach has been extensively used to investigate photoelectron emission from atomic targets [21,22] and more recently from surfaces [17,18]. The induced potential is derived from a linear response theory by using a one-dimensional jellium model [23]. It can be expressed as $V_{\text{ind}}(z,t) = zg(t)$ inside the solid, with the function $g(t)$ numerically determined, while outside the solid—in the vacuum region—$V_{\text{ind}}(z,t) = 0$. Hence, the final SJV wave function can be written as

$$\chi_f^{(\text{SJV})-}(\mathbf{r},t) = \Phi_{\mathbf{k}_f}^{-}(\mathbf{r},t)\exp[iD_L^{-}(k_{fz},z,t)]\xi_{\text{ind}}(z,t), \tag{5}$$

where $\Phi_{\mathbf{k}_f}^{-}(\mathbf{r},t)$ is the unperturbed final state given by Eq. (2), which includes the asymptotic condition corresponding to emission towards the vacuum zone (external ionization process [20]). In Eq. (5), the function D_L^{-} represents the Volkov phase associated with the laser field, which is expressed as

$$D_L^{-}(k_{fz},z,t) = \frac{z}{c}A^{-}(t) - \beta^{-}(t) - k_{fz}\alpha^{-}(t). \tag{6}$$

The temporal functions involved in Eq. (6) are the vector potential $A^{-}(t)$, which represents the momentum transferred by the electric field, the ponderomotive energy $\beta^{-}(t)$, associated with the kinetic energy gained by the electron due to the interaction with the laser, and the quiver amplitude $\alpha^{-}(t)$, corresponding to the classical oscillation amplitude of the electron in the presence of the laser field. These magnitude are defined as

$$A^{-}(t) = -c\int_{+\infty}^{t} dt' F(t'),$$

$$\beta^{-}(t) = (2c^2)^{-1}\int_{+\infty}^{t} dt'[A^{-}(t')]^2,$$

$$\alpha^{-}(t) = c^{-1}\int_{+\infty}^{t} dt' A^{-}(t'), \tag{7}$$

with c the speed of light. In a similar way we express the function ξ_{ind}, which considers the action of the induced potential on the active electron, as

$$\xi_{\mathrm{ind}}(z,t)=\begin{cases}\exp[i(z/c)A_{\mathrm{ind}}^{-}(t)] & \text{for } z\leqslant 0\\ 1 & \text{for } z>0\end{cases}, \tag{8}$$

with $A_{\mathrm{ind}}^{-}=-c\int_{+\infty}^{t}dt'g(t')$ the momentum transferred by the induced field. Note that the effect of the image charge of the emitted electron was not taken into account in the final distorted wave function $\chi_f^{(\mathrm{SJV})-}$ because its contribution has been found negligible in previous calculations [24].

Employing the final SJV wave function given by Eq. (5) within a time-dependent distorted-wave formalism [25], the transition amplitude reads as

$$T_{if}^{(\mathrm{SJV})}=T^{(\mathrm{C})}+T^{(\mathrm{PC})}, \tag{9}$$

where

$$T^{(\mathrm{C})}=-i\int_0^{\tau}dt\langle\chi_f^{(\mathrm{SJV})-}(t)|U(t)|\Phi_{\mathbf{k}_i}^{+}(t)\rangle \tag{10}$$

represents the primary or collision (C) term, with $U(z,t)=V_L(z,t)+V_{\mathrm{ind}}(z,t)$ the perturbation introduced by the laser and the induced fields and $\Phi_{\mathbf{k}_i}^{+}$ the unperturbed initial state, given by Eq. (2). The second term of Eq. (9), $T^{(\mathrm{PC})}$, is here called the postcollision (PC) transition amplitude, corresponding to the emission process after the pulse turns off at the time τ. It reads as

$$T^{(\mathrm{PC})}=-i\int_{\tau}^{+\infty}dt\langle\chi_f^{(\mathrm{SJV})-}(t)|V_{\mathrm{ind}}(t)|\Phi_{\mathbf{k}_i}^{+}(t)\rangle. \tag{11}$$

B. TDSE Solution

Replacing the semi-infinite jellium potential by the one corresponding to a one-dimensional slab of size a, $V_{\mathrm{slab}}=-V_c\Theta(a/2-z)\Theta(a/2+z)$, and taking into account the symmetry of the system in the direction parallel to the surface, we can write the unperturbed eigenstates as

$$\Phi_{\mathbf{k},n}(\mathbf{r},t)=\frac{e^{i\mathbf{k}_s\cdot\mathbf{r}_s}}{2\pi}\phi_n(z)e^{-iE_{\mathbf{k}}t}, \tag{12}$$

where now the functions $\phi_n(z)$ are the discretized one-dimensional eigenstates of the slab potential.

The time evolution of the electronic eigenstates under the laser pulse perturbation is governed by the one-dimensional time-dependent Schrödinger equation

$$i\frac{\partial}{\partial t}\phi_n(z,t)=H(z,t)\phi_n(z,t), \tag{13}$$

where the unperturbed part of the Hamiltonian $H(z,t)$ is now $H_0=-(1/2)(d^2/dz^2)+V_{\mathrm{slab}}$.

The discrete time step evolution is given by the evolution operator

$$\phi_n(z,t+\Delta t)=\exp(-i\Delta tH)\phi_n(z,t), \tag{14}$$

which is computed by using the Crank–Nicholson scheme, approximating the exponential by the Cayley form [26],

$$\exp(-i\Delta tH)\approx\frac{1-\frac{i\Delta t}{2}H}{1+\frac{i\Delta t}{2}H}. \tag{15}$$

This scheme is unitary, unconditionally stable, and accurate up to order $(H\Delta t)^2$.

To obtain the transition amplitude we evolve every eigenstate within the Fermi sphere of the unperturbed slab, then projecting the evolved states over the discretization box continuum states, $\phi_f^k(z)$,

$$T_{if}^{(\mathrm{TDSE})}=\langle\phi_f^k(z)|\phi_i(z,t\to\infty)\rangle. \tag{16}$$

The independence of the results with respect to different slab sizes guarantees that the slab size used accurately represents the semi-infinite medium.

3. RESULTS

We applied the SJV and TDSE methods to study electron emission from the valence band of an Al(111) surface produced as a consequence of grazing-incidence ultrashort and intense laser pulses. As Al is a typical metal surface, it will be considered a benchmark for the theory. The Al(111) is described by the following parameters: the Fermi energy $E_F=0.414$ a.u., the work function $E_W=0.156$ a.u., and the surface plasmon frequency $\omega_s=0.4$ a.u..

For the TDSE calculations a slab with a width of 311.54 a.u. (142 Al atomic layers), surrounded by 244.23 a.u. of vacuum on each side, was used in order to get enough resolution in the continuum momentum space. The grid sizes were $\Delta z=0.1$ a.u. for the spacial grid and $\Delta t=0.005$ a.u. for the time grid. The time evolution was considered finished when the induced potential had decayed 2 orders of magnitude from its value at the moment the laser pulse was switched off, at $t=\tau$. The same criterion was used to evaluate the upper limit of the time integral of Eq. (11). Note that to compare the SJV and TDSE results it is necessary to take into account that the former theory includes the proper asymptotic conditions, distinguishing the external from the internal ionization processes, while the latter does not. Then, as a first estimation we weighted TDSE values with the fraction of electrons emitted toward the vacuum derived from the SJV model [16]. This technique was successfully applied to the problem of ions grazing metal surfaces [27].

In this work we considered symmetric pulses, with $\phi=-\omega\tau/2+\pi/2$. The field strength was fixed as $F_0=0.001$ a.u. ($I\simeq 4\cdot10^{10}$ W/cm^2), which belongs to the perturbative regime, far from the saturation region and the damage threshold, in accord with experimental values [9,12,28,29]. Taking into account the results of a previous theory [16], the maximum of the emission probability corresponds to the angle $\theta_e=90°$, which coincides with the orientation of the laser field. Therefore, all results presented here refer to this emission angle.

Since the dynamic response of the surface is characterized by the surface plasmon frequency ω_s, in order to investigate the influence of the induced potential we varied

the carrier frequency ω of the laser field around the value of ω_s. We start by considering laser pulses with several oscillations inside the envelope function, which correspond to the so-called multiphoton regime. In this regime, related to a Keldysh parameter $\gamma=\omega\sqrt{E_W}/F_0$ [30] greater than the unity, the laser frequency tends to the photon energy, and the electron spectrum displays maxima associated with the absorption of photons.

In Fig. 1, six-cycle laser pulses with three different frequencies were considered: $\omega=0.7, 0.4, 0.2$ a.u.. In all cases, to analyze the effect of the surface response on the electronic spectra, SJV and TDSE values were compared with data derived within the previous IJV approach [16], which neglects the contribution of V_{ind}. In Fig. 1(a) we show the emission probability corresponding to the frequency $\omega=0.7$ a.u., which is higher than the surface plasmon frequency. For this frequency a good agreement between SJV and TDSE results is found. The SJV curve runs very close to TDSE values, showing only a small underestimation of TDSE results in the high-velocity range. Both theories present a broad maximum that can be associated with the above threshold ionization process, corresponding to electron emission by absorption of one photon. Note that the width of this peak decreases as the duration of the pulse increases; that is, for a given number of cycles (six cycles in our case) the peak width diminishes for decreasing laser frequencies, as was also observed in the atomic case [31]. From the comparison with values obtained within the IJV approximation, we observe that for this high frequency the induced potential produces only a slight increase of the probability at low electron energies, having a minor influence on the overall electronic spectrum. However, when ω becomes resonant with the surface plasmon frequency, as in Fig. 1(b), the induced potential contributes greatly to increase the ionization probability in the whole energy range. Energy distributions obtained with SJV and TDSE methods are more than 1 order of magnitude higher than the one derived from the IJV approach. In this case SJV results follow the behavior of the TDSE curve quantitatively well, properly describing the positions of the multiphoton maxima but underestimating TDSE probabilities around the second peak. In Fig. 1(c) we plot the emission probability for a laser field with a frequency $\omega=0.2$ a.u., lower than the plasmon one. Again, as in Fig. 1(a), SJV and TDSE results run very close to each other, displaying almost no differences with the IJV theory, which does not contain the induced potential. This indicates that the induced potential strongly affects emission spectra for frequencies resonant with the surface plasmon frequency, while for small deviations from this frequency it plays a minor role in the multiphoton ionization process. Notice that in the resonant case, $\omega=\omega_s$, the contribution of the plasmon decay mechanism should be also included, producing an additional superimposed structure just at the electronic energy ω_s [32].

With the aim of examining in detail the contribution of the induced potential, in Fig. 2 we plot V_{ind} as a function of time, for a given position inside the solid and for the frequencies of Figs. 1(a) and 1(b). We observe that for $\omega=0.7$ a.u. the induced potential tends to follow the oscilla-

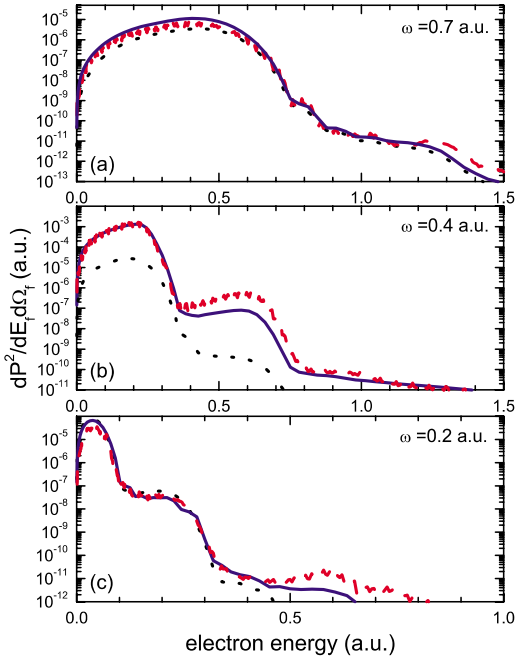

Fig. 1. (Color online) Differential electron emission probability for six-cycles pulses, as a function of the electron energy, for the emission angle $\theta_e=90°$. The parameters of the laser field are $F_0=0.001$ a.u., (a) $\omega=0.7$ a.u., $\tau=54$ a.u., (b) $\omega=0.4$ a.u., $\tau=95$ a.u., and (c) $\omega=0.2$ a.u., $\tau=190$ a.u.. Solid, dashed, and dotted curves show values evaluated with SJV, TDSE, and IJV models, respectively.

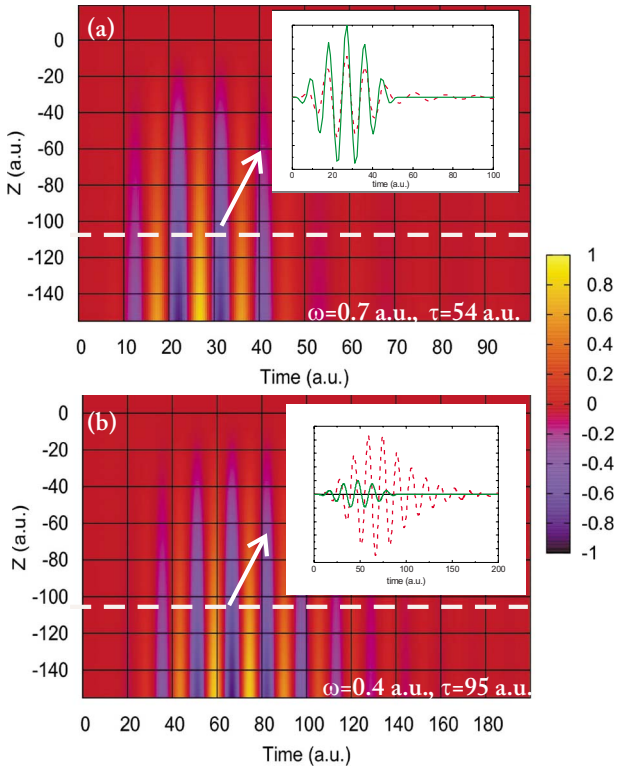

Fig. 2. (Color online) Two-dimensional representation of the induced potential, as a function of time and distance z perpendicular to the surface, with $z=0$ the edge of the surface. Laser pulse parameters are similar to Figs. 1(a) and 1(b). Insets correspond to a given position inside the solid, with the solid curve the laser pulse and the dashed curve the induced potential.

tions of the external field, and its intensity steeply diminishes when the pulse is turned off. Then, in this case the collective response of the medium produces only a weak effect on the electronic spectrum, as shown in Fig. 1(a). Whereas for laser frequencies near ω_s [Fig. 2(b)] the process is dominated by the induced potential, which produces an increment of the emission probability, as observed in Fig. 1(b).

Finally, in Fig. 3 we study a six-cycle laser pulse with the frequency corresponding to the experimental value for the Ti:sapphire laser system [9] (ω=0.057 a.u.). For this low frequency, almost 1 order of magnitude lower than the plasmon one, the surface response approximates the static limit, and electronic fluctuations strongly screen the external field inside the solid. By comparing SJV and IJV results it is observed that in this case the induced potential contributes to reduce the emission probability markedly, up to 2 orders of magnitude at low electron energies. On the other hand, it should be noted that although the SJV theory properly describes the positions of multiphotonic maxima, it overestimates the emission probability given by the TDSE method. Such a discrepancy, which arises when ω is lower than the mean energy of initial bound electrons, was also observed for other Volkov-type methods applied to photoionization of atomic targets [21].

To complete the previous analysis we reduce the duration of the pulse in order to investigate the contribution of the induced potential for photoelectron emission in the collisional regime [21]. In this regime, associated with half-cycle pulses, the electromagnetic field does not oscillate, producing a perturbation similar to the one resulting of the interaction with a swift ion impinging grazingly on the surface (collision process). Notice that for such ultrashort pulses the carrier frequency ω loses its meaning, and the pulse can be characterized by the sudden momentum transferred to the ejected electron, $\Delta p = -A^{-}(0)/c \simeq F_0\tau/2$ [22]. In Fig. 4 we plot electron distributions for half-cycle pulses with two different durations τ=4.5 a.u. and τ=16 a.u.. In both cases we found good agreement between SJV and TDSE methods over the whole electron velocity range. Both theories present a pronounced maximum at low electron velocities, which does not appear in the electron distribution derived from the IJV approach, as it is produced by the induced potential. To understand the origin of this increment of the probability at low electron energies, in Fig. 5 we again plot the induced potential for a given position inside the solid, but now for the case of Fig. 4(a). We observe that for half-cycle pulses, without oscillations, after the pulse has finished the induced potential still affects solid electrons during at least more 100 a.u. This effect is the main source of electron emission at low velocities.

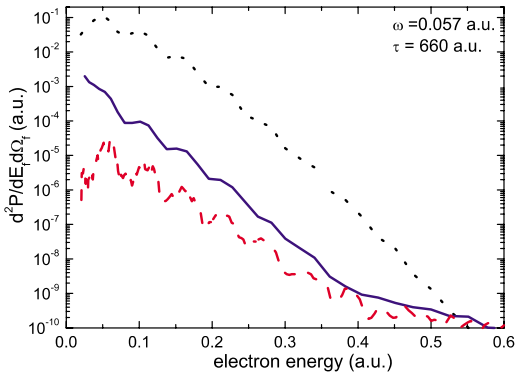

Fig. 3. (Color online) Similar to Fig. 1. Laser field with F_0 =0.001 a.u., frequency ω=0.057 a.u. and duration τ=660 a.u..

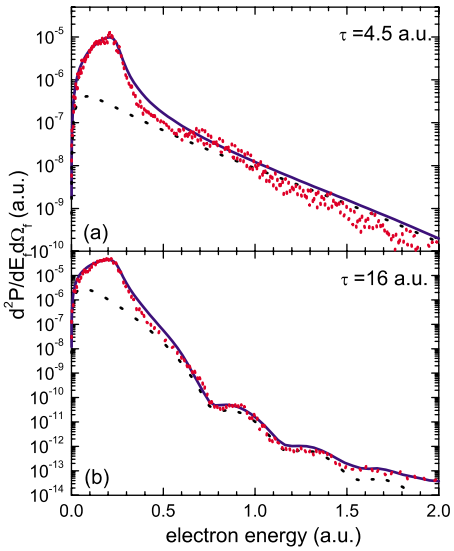

Fig. 4. (Color online) Similar to Fig. 1. Half-cycle pulse with F_0=0.001 a.u., (a) frequency ω=0.7 a.u., and duration τ =4.5 a.u.; (b) frequency ω=0.2 a.u. and duration τ=16 a.u..

4. CONCLUSIONS

In the present work we have introduced the SJV approximation, which allowed us to investigate the effects of the induced potential on the electron emission process. The proposed theory was compared with values derived from the numerical solution of the corresponding TDSE, displaying a good description of the main characteristics of photoemission spectra in the whole range of studied frequencies and durations of the laser pulse. From the comparison between SJV probabilities and those derived from the previous IJV approach, which does not include V_{ind}, we conclude that the induced potential can play an important role in laser-induced electron emission from metal surfaces, as expected. For laser pulses with several oscillations inside the envelope, we found that the induced potential produces a considerable increment of the probability when the laser frequency is resonant with the surface

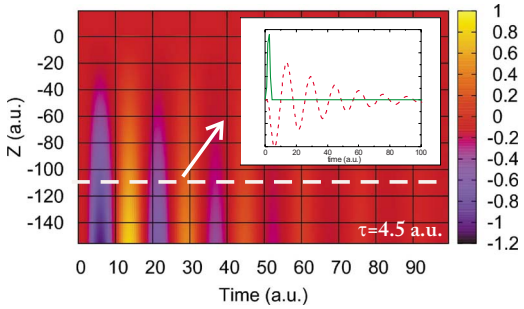

Fig. 5. (Color online) Similar to Fig. 2. Laser field with F_0 =0.001 a.u., ω=0.7 a.u., and τ=4.5 a.u..

plasmon one, but as ω diminishes, tending to the static case, the surface electronic density shields the laser field inside the solid, leading to a marked reduction of the photoemission process. In addition, for electromagnetic pulses in the collisional regime, the contribution of the surface induced potential after the pulse turns off gives rise to a maximum in the emission spectrum at low energies.

ACKNOWLEDGMENT

This work was done with the financial support of grants UBACyT, ANPCyT and CONICET of Argentina. I. Aldazabal, A. Arnau, and V. Silkin gratefully acknowledge financial support by GV-UPV/EHU (grant IT-366-07) and MCI (grant FIS2007-66711-C02-01).

REFERENCES

1. A. L. Cavalieri, N. Müller, Th. Uphues, V. S. Yakovlev, A. Baltuska, B. Horvath, B. Schmidt, L. Blümel, R. Holzwarth, S. Hendel, M. Drescher, U. Kleineberg, P. M. Echenique, R. Kienberger, F. Krausz, and U. Heinzmann, "Attosecond spectroscopy in condensed matter," Nature **449**, 1029–1032 (2007).
2. E. Goulielmakis, V. S. Yakovlev, A. L. Cavalieri, M. Uiberacker, V. Pervak, A. Apolonski, R. Kienberger, U. Kleineberg, and F. Krausz, "Attosecond control and measurement: lightwave electronics," Science **317**, 769–775 (2007).
3. R. Kienberger, E. Goulielmakis, M. Uiberacker, A. Baltuska, V. Yakovlev, F. Bammer, A. Scrinzi, Th. Westerwalbesloh, U. Kleineberg, U. Heinzmann, M. Drescher, and F. Krausz, "Atomic transient recorder," Nature **427**, 817–821 (2004).
4. C. A. Haworth, L. E. Chipperfield, J. S. Robinson, P. L. Knight, J. P. Marangos, and J. W. G. Tisch, "Half-cycle cutoffs in harmonic spectra and robust carrier-envelope phase retrieval," Nat. Phys. **3**, 52–57 (2007).
5. A. Baltuska, Th. Udem, M. Uiberacker, M. Hentschel, E. Goulielmakis, Ch. Gohle, R. Holzwarth, V. S. Yakovlev, A. Scrinzi, T. W. Hänsch, and F. Krausz, "Attosecond control of electronic processes by intense light fields," Nature **421**, 611–615 (2003).
6. E. Lorin, S. Chelkowski, and A. D. Bandrauk, "Attosecond pulse generation from aligned molecules-dynamics and propagation in H_2^+," New J. Phys. **10**, 025033 (2008).
7. D. B. Milošević, G. G. Paulus, D. Bauer, and W. Becker, "Above-threshold ionization by few-cycle pulses," J. Phys. B **39**, R203–R262 (2006).
8. M. F. Kling, J. Rauschenberger, A. J. Verhoef, E. Hasovic, T. Uphues, D. B. Milošević, H. G. Muller, and M. J. J. Vrakking, "Imaging of carrier-envelope phase effects in above-threshold ionization with intense few-cycle laser fields," New J. Phys. **10**, 025024 (2008).
9. L. Miaja-Avila, G. Saathoff, S. Mathias, J. Yin, C. La-o-vorakiat, M. Bauer, M. Aeschlimann, M. M. Murnane, and H. C. Kapteyn, "Direct measurements of core-level relaxation dynamics on a surface-adsorbates system," Phys. Rev. Lett. **101**, 046101 (2008).
10. A. K. Kazansky and P. M. Echenique, "One-electron model for the electronic response of metal surfaces to subfemtosecond photoexcitation," Phys. Rev. Lett. **102**, 177401 (2009).
11. C. Lemell, B. Solleder, K. Tőkési, and J. Burgdörfer, "Simulation of attosecond streaking of electrons emitted from a tungsten surface," Phys. Rev. A **79**, 062901 (2009).
12. M. I. Stockman, M. F. Kling, U. Kleineberg, and F. Krausz, "Attosecond nanoplasmonic-field microscope," Nat. Photonics **1**, 539–544 (2007).
13. A. Kubo, K. Onda, H. Petek, Z. Sun, Y. S. Jung, and H. K. Kim, "Femtosecond imaging of surface plasmon dynamics in a nanostructured silver film," Nano Lett. **5**, 1123–1127 (2005).
14. D. M. Volkov, "About a class of solutions of the Dirac equation," Z. Phys. **94**, 250–260 (1935).
15. F. H. M. Faisal, J. Z. Kamiński, and E. Saczuk, "Photoemission and high-order harmonic generation from solid surfaces in intense laser fields," Phys. Rev. A **72**, 023412 (2005).
16. M. N. Faraggi, M. S. Gravielle, and D. M. Mitnik, "Interaction of ultrashort laser pulses with metal surfaces: impulsive jellium–Volkov approximation versus the solution of the time-dependent Schrödinger equation," Phys. Rev. A **76**, 012903 (2007).
17. J. C. Baggesen and L. B. Madsen, "Theory of time-resolved measurements of laser-induced electron emission from metal surfaces," Phys. Rev. A **78**, 032903 (2008).
18. C.-H. Zhang and U. Thumm, "Attosecond photoelectron spectroscopy of metal surfaces," Phys. Rev. Lett. **102**, 123601 (2009).
19. M. S. Gravielle and J. E. Miraglia, "Energy and electron spectra after grazing-ion-surface collisions," Phys. Rev. A **65**, 022901 (2002).
20. M. S. Gravielle, "Binary mechanism in grazing ion-surface collisions," Phys. Rev. A **58**, 4622–4629 (1998).
21. P. Macri, J. E. Miraglia, and M. S. Gravielle, "Ionization of hydrogen targets by short laser pulses," J. Opt. Soc. Am. B **20**, 1801–1806 (2003).
22. D. G. Arbó, K. Tőkési, and J. E. Miraglia, "Atomic ionization by a sudden momentum transfer," Nucl. Instrum. Methods Phys. Res. B **267**, 382–385 (2009).
23. M. Alducin, V. M. Silkin, J. I. Juaristi, and E. V. Chulkov, "Energy loss of ions at metal surfaces: band-structure effects," Phys. Rev. A **67**, 032903 (2003).
24. P. Dombi, F. Krausz, and G. Farkas, "Ultrafast dynamics and carrier-envelope phase sensitivity of multiphoton photoemission from metal surfaces," J. Mod. Opt. **53**, 163–172 (2006).
25. D. P. Dewangan and J. Eichler, "Charge exchange in energetic ion-atom collisions," Phys. Rep. **247**, 59–219 (1994).
26. W. H. Press, S. A. Teukolsky, W. T. Vetterling, and B. P. Flannery, *Numerical Recipes* (Cambridge Univ. Press, 1992).
27. M. N. Faraggi, M. S. Gravielle, and V. M. Silkin, "Quantum-mechanical model for valence-electron emission from metal surfaces," Phys. Rev. A **69**, 042901 (2004).
28. G. Saathoff, L. Miaja-Avila, M. Aeschlimann, M. M. Murnane, and H. C. Kapteyn, "Laser-assited photoemission from surfaces," Phys. Rev. A **77**, 022903 (2008).
29. L. Miaja-Avila, J. Yin, S. Backus, G. Saathoff, M. Aeschlimann, M. M. Murnane, and H. C. Kapteyn, "Ultrafast studies of electronic processes at surfaces using the laser-assisted photoelectric effect with long-wavelength dressing light," Phys. Rev. A **79**, 030901(R) (2009).
30. L. V. Keldysh, "Ionization in the field of a strong electromagnetic wave," Sov. Phys. JETP **20**, 1307–1314 (1965).
31. V. D. Rodríguez, E. Cormier, and R. Gayet "Ionization by short UV laser pulses: secondary above-threshold-ionization peaks of the electron spectrum investigated through a modified Coulomb–Volkov approach," Phys. Rev. A **69**, 053402 (2004).
32. G. Bocan and J. E. Miraglia, "Electron excitation after plasmon decay in proton–aluminum collisions," Phys. Rev. A **67**, 032902 (2003).